2 mif

X-621-74-138
PREPRINT

ION EFFECTS ON IONOSPHERIC ELECTRON RESONANCE PHENOMENA

ROBERT F. BENSON

MAY 1974

GSFC — GODDARD SPACE FLIGHT CENTER —
GREENBELT, MARYLAND

X-621-74-138
Preprint

ION EFFECTS ON IONOSPHERIC ELECTRON RESONANCE PHENOMENA

by

Robert F. Benson

Laboratory for Planetary Atmospheres

Goddard Space Flight Center

May 1974

Goddard Space Flight Center

Greenbelt, Maryland

ABSTRACT

Ion effects are often observed on topside-sounder stimulated electron plasma wave phenomena. A commonly observed effect is a spur, appearing after a time delay corresponding to the proton gyro period, attached to the low frequency side of an electron plasma resonance. The spurs are often observed on the resonances at the electron plasma frequency f_N, the harmonics nf_H of the electron cyclotron frequency f_H ($n = 2, 3, 4, \cdots$), and occasionally on the upper hybrid frequency $(f_N^2 + f_H^2)^{1/2}$. The spurs on the f_N resonance are usually quite small unless the f_N resonance overlaps with an nf_H resonance; very large spurs are observed during such overlap conditions. Proton spurs are only observed on the nf_H resonances when the electron plasma waves associated with these resonances are susceptible to the Harris instability and when the electromagnetic z wave can be initiated by the sounder pulse. This instability is the result of a sounder stimulated anisotropic electron velocity distribution. The observations suggest that energy is fed into the nf_H longitudinal plasma wave from the z wave via wave-mode coupling. The magnitude of the nf_H spurs for large n is much greater than for small n.

INTRODUCTION

When a pulsed rf transmitter operates from a spacecraft in the ionosphere, plasma waves associated with longitudinal electron oscillations can be stimulated. These electron plasma waves have been labeled as resonances because they are observed immediately after the pulse transmission and can persist for a time period which is several orders of magnitude greater than the pulse duration. The resonant phenomena have been observed and extensively studied using a series of topside sounder satellites. These studies have provided information on the ambient values for the electron density N, the electron temperature T, and the strength of the magnetic field B. In addition, instabilities and non-linear phenomena associated with the propagation of electron plasma waves have been investigated. A recent review of the topside sounder resonance phenomena has been given by Muldrew (1972).

It is customary in the interpretation of the plasma resonance phenomena to ignore the motion of the ions, because of their large mass, and to consider only the longitudinal oscillations of the electrons. Under certain conditions, however, ion effects are observed and a proper interpretation of these effects will have to include ion motions. Three different effects have been reported:

(1) Graff (1967) detected an amplitude modulation with a period equal to the proton cyclotron gyration period τ_p superimposed on the resonance observed at the electron plasma frequency f_N on Alouette 2 data.

(2) King and Preece (1967) detected spurs on Alouette I electron resonance phenomena which appear at time delays equal to multiples of τ_p.

(3) Matuura and Nishizaki (1969) detected short time duration echoes at multiples of τ_p on Alouette 2 ionograms. The echoes were most often observed between the electron cyclotron frequency f_H and f_N and they were not attached to the electron resonance phenomena.

Palmer and Barrington (1973) observed emissions at a few kilohertz with the ISIS 2 VLF receiver which were stimulated by the ISIS 2 sounder transmitter operating at a few megahertz. These emissions often revealed a modulation with a period equal to τ_p.

The purpose of the present paper is to provide observational evidence concerning ion effects of the spur type which suggests that the phenomena may involve electromagnetic-electrostatic wave-mode coupling and plasma wave instabilities stimulated by the sounder pulse.

OBSERVATIONS

The observations were taken during 8 different passes of the Alouette 2 satellite. The data were selected in a manner that would provide continuous sequences of ionograms with a nearly fixed frequency pattern of nf_H resonances ($n = 2, 3, 4\cdots$) and a rapidly changing pattern of the resonant and cut-off

phenomena that are dependent on N, i.e., the resonances at f_N and the upper-hybrid frequency f_T ($f_T^2 = f_N^2 + f_H^2$) and the cut-off frequencies at the position of the satellite $f_Z S$ and $f_X S$, for the electromagnetic z and x traces, respectively. The geographic latitude-longitude tracks for all of the passes used in the present study are similar to those shown in Figure 1 of Benson (1972b).

Small spurs are often observed on the f_N resonance. Figure 1 shows an f_N resonance with three clear spurs (and the beginning of a fourth), each separated by the ambient value of τ_p. The spurs are more pronounced when they are observed on the nf_H resonances. Figure 2 shows a $3f_H$ resonance with two spurs, again separated by τ_p. The spurs are almost always observed only on the low frequency side of the resonance. Exceptions, such as the one shown in Figure 3, can be attributed to the wide sounder bandwidth (see Appendix). The spur overshoot to the high frequency side of the $4f_H$ resonance in this illustration can be seen on the ionogram format and even more clearly on the receiver amplitude vs. time format (see inserts g and h). This high frequency overshoot is not merely an extension of the spur on the f_N resonance because 2 receiver amplitude traces are observed with no spur after the h trace of the insert in Figure 3 and before the f_N spur appears. The largest spurs of all are observed during conditions in which the f_N resonance overlaps with an nf_H resonance. A striking example of this condition is given in Figure 4 where a large spur is observed on the combined $2f_H/f_N$ resonance.

In order to record the extent of the spurs observed on the f_N, f_T, and nf_H resonances, the minimum frequency f_{min} attained by the principal spur, i.e., the

one observed after a delay time τ_p, was scaled. The location of f_{min} coincides with the scan line identified as (a) in Figure 4. The f_{min} values, normalized by f_H are presented as a function of the plasma parameter f_N/f_H in Figure 5; f_N and f_H were determined from the resonant and cut-off phenomena on the ionograms containing the spurs. In this figure, the conditions for the $2f_H$ through the $7f_H$ resonances are indicated by horizontal lines and the conditions for the f_N and f_T resonances are indicated by the dashed slanting lines. Points very close to a resonant line indicate very small spurs. For example, the N's (which represent spurs on the f_N resonance) are very close to the $f_{min} = f_N$ line for low values of f_N/f_H; this line corresponds to the condition of no spur. Similarly, points far below the resonance line indicate large spurs, e.g., the lowest open circles near $f_N/f_H \approx 3$ correspond to spurs on the combined f_N and $3f_H$ resonance which extend well into the frequency region below the midway point between $2f_H$ and $3f_H$. The concentration of spur observations in the region to the left of $f_N/f_H \approx 4$ is the result of a concentration of data corresponding to this plasma condition as can be seen from the histogram of Figure 6. The main features to note in Figure 5 are the following:

1. Spurs are only observed when $f_Z S > f_H$.
2. Spurs are often observed on the f_N and nf_H resonances ($n = 2, 3, 4, \cdots$) and occasionally on the f_T resonance.
3. Spurs are observed on the f_N resonance over the entire frequency range between the harmonics of f_H.

4. The minimum frequency of the f_N spur is about 5% below the value of f_N; the least square straight line fit to the f_N spur data points yields

$$f_{min}/f_H = 0.959\,(f_N/f_H) - 0.022\,.$$

with a correlation coefficient of 0.999.

5. The spurs associated with the f_N resonance are observed to cover a much wider frequency range when the f_N resonance overlaps with an nf_H resonance.

6. In general, the spurs on the nf_H resonances appear to be confined in frequency to the vicinity of $f_Z S$ with spurs being observed further to the left of the $f_Z S = nf_H$ condition ($f_Z S < nf_H$) than to the right of this condition ($f_Z S > nf_H$). The major exception is the group of $2f_H$ spurs observed when $f_N/f_H \approx 3$.

7. The spurs on the nf_H resonances rarely extend into the frequency region below the midway point between nf_H and $(n-1)f_H$. The exceptions are attributed to instrumental effects (see appendix).

8. The 3 cases of spurs associated with the f_T resonance (2 near $f_N/f_H = 1.5$ and 1 near $f_N/f_H = 3.5$) are also confined to the above frequency region.

9. The largest of the nf_H spurs are observed for large n. (Only 2 of the 9 spurs with $n \geq 4$ approach the region within 20% of the resonance line whereas 24 of the 27 $3f_H$ spurs are confined to this region.)

The minimum value for the f_{min}/f_H scale was taken as 1 rather than zero in Figure 5 because proton spurs have never been observed on the resonance at f_H. Even when the conditions of point 6 above are satisfied with n = 1, spurs are not observed on this resonance. An example of the indifference of the f_H resonance to the location of $f_Z S$ is given in Figure 7 where 4 consecutive ionograms corresponding to the plasma conditions $f_Z S < f_H$ to $f_Z S > f_H$ are presented. The anomalous behavior of the $2f_H$ spur mentioned in point 6 is illustrated in Figure 8a where $f_N/f_H = 3.02$. The spur appears as a diffuse patch attached to the low frequency side of the $2f_H$ resonance; it covers a wide time delay interval of approximately 2 msec with the minimum delay (the top of the spur) corresponding to τ_p. This appearance is typical of all $2f_H$ spurs observed when $f_Z S > 2f_H$ (the solid points near $f_N/f_H = 3$ in Figure 5). The $2f_H$ spurs observed when $f_Z S < 2f_H$ (the 3 solid points near $f_N/f_H \approx 2.2$) have a more normal form, i.e., well defined traces of short time duration (less than 1 msec) near the f_{min} point. This form of the $2f_H$ spur is seldom observed, whereas a well defined $3f_H$ spur is almost always observed when $f_Z S \lesssim 3f_H$. (The number of ionograms scaled in the f_N/f_H range from 3.2 to 3.6 is only a little over 20% greater than the number in the 2.2 to 2.6 range [see Figure 6], yet the solid points in Figure 5 indicate that there are more than 8 times as many $3f_H$ spurs observed than $2f_H$ spurs in the respective f_N/f_H ranges). An investigation of the Alouette 1 ionograms used by King and Preece (1967) reveals that most of their spurs were either associated with the combined $f_N/3f_H$ resonance (as in Figure 8a) or the $3f_H$ resonance (as in Figures 2, 8b, and 8c).

The 9 consecutive ionograms presented in Figures 8a-8i illustrate typical resonance and spur characteristics as the plasma parameter f_N/f_H changes from 3.0 to 6.2. With the exception of $2f_H$ (discussed above), spurs are only observed on the nf_H resonances when $f_Z S$ is in the vicinity of nf_H. When the f_N resonance is observed separate from the other resonances it either has weak spurs (as in Figure 8c, 8e, and 8g or spurs are not observed (as in Figure 8i); when it overlaps with an nf_H resonance strong spurs are observed on the combined resonance (as in Figures 8a, 8d, 8f, and 8h). The nf_H resonances showing spurs when $f_Z S \lesssim nf_H$ are usually greatly enhanced. For example, compare the duration and frequency width of the $6f_H$ resonance of Figure 8i with the earlier ionograms where an unobstructed $6f_H$ resonance is observed, i.e., all ionograms except the one in Figure 8h where f_N overlaps with $6f_H$. The $3f_H$ resonance shows a singular behavior in that it completely disappears in the high frequency portion of the emerging diffuse resonance signal between $2f_H$ and $3f_H$ when $f_N/f_H \approx 4$. This behavior is illustrated in Figure 8d – the only ionogram of the series with no $3f_H$ resonance.

The large magnitude of the spurs corresponding to large n is illustrated in Figure 8i for $n = 6$ (note the compressed frequency scale above 2.0 MHz) and again for $n = 5$ and 6 in Figure 9. The $5f_H$ spur of Figure 9a is seen to be a major appendage to the relatively narrow bandwidth resonance signal. The second spur (i.e., at $2\tau_p$) on the $6f_H$ resonance of Figure 8i blossoms out just as the resonance signal is fading away. A similar behavior is observed for the τ_p spur on the $6f_H$ resonance of Figure 9b.

Ion effects are also observed with the diffuse resonances. These effects, however, have a different appearance than the spurs described above. For example, Figure 10 shows a weak signal corresponding to the time delay τ_p protruding on each side of the f_{D1} diffuse resonance. Figure 11 shows a proton signal protruding from the low frequency side of the f_{DII} resonance and extending to the f_{D1} resonance. These examples are typical of the type of proton signals that are observed with the electron diffuse resonances.

DISCUSSION

There are two features concerning the observations of proton spurs on the nf_H resonances which suggest that the phenomena may be related to the stimulation of plasma wave instabilities of the type first discussed by Harris (1959). [The Harris instability is the result of an anisotropic electron velocity distribution with $T_\perp > T_{||}$ where $T_\perp$ and $T_{||}$ are the temperatures corresponding to electron motion perpendicular and parallel to $\vec{B}$, respectively. The anisotropy is stimulated by the cyclotron damping of the plasma waves generated by the sounder pulse. Previous studies have indicated that the energy absorbed is sufficient to produce the instability for the waves associated with the sequence of diffuse resonances at f_{Dn} (Oya, 1971) and the nf_H resonances with n = 2, 3, 4, . . . (Benson, 1974a)]. These features (designated as numbers 6 and 7 in connection with the discussion of Figure 5) are the importance of the location of the cutoff of the electromagnetic z trace, and the restriction of the nf_H spur observations to the frequency region between nf_H and the mid-point between nf_H and $(n-1)f_H$.

It is instructive to consider the dispersion curves for plasma waves propagating nearly perpendicular to $\vec{B}$ in connection with these observations. [The resonances at nf_H with $n = 2, 3, 4, \cdots$ are attributed to such plasma waves which are stimulated by the sounder pulse (see the review by Muldrew, 1972).] The dispersion curves corresponding to the observations of Figure 2 are presented in Figure 12. The cutoff frequencies f_ZS and f_XS for the electromagnetic z and x waves are indicated on the ordinate axis together with the location of the ambient upper-hybrid frequency. The shaded regions correspond to the frequency domains where the Harris instability can be stimulated for oblique propagation (Harris, 1964; Shima and Hall, 1965). The nf_H resonances with $n = 2, 3, 4, \cdots$ are attributed to waves corresponding to the portion of the dispersion curve very near nf_H with small kR values (see review by Muldrew, 1972). Thus the wave associated with the $3f_H$ resonance is in an unstable region whereas the wave associated with the $4f_H$ resonance is in a stable region. As f_N increases, f_ZS and f_XS pass through $3f_H$ and $4f_H$, respectively. The $3f_H$ wave remains in the unstable region during this transition, whereas the $4f_H$ wave remains stable. This situation is true for each of the nf_H resonances ($n = 2, 3, 4, \cdots$) i.e., the plasma wave corresponding to low kR near nf_H can experience the Harris instability when $f_ZS \approx nf_H$ but not when $f_XS \approx nf_H$.

While the observations of Figure 5 suggests that the presence of the Harris instability is a necessary condition for the generation of proton spurs on the nf_H resonances, it is not a sufficient condition. This is true because the plasma

waves associated with a given nf_H resonance can be unstable in the frequency domain between nf_H and $nf_H - f_H/2$ in the entire region to the right of the dashed line labeled f_T in Figure 5. Proton spurs are only observed, however, in the vicinity of $f_Z S = nf_H$. The spread of data points around $f_Z S = nf_H$ is attributed to the wide frequency spectrum of the transmitted sounder pulse (see appendix). Thus spurs are only observed when the passband of the receiver includes signals from the frequency region where the Harris instability can be stimulated, and when sufficient energy is transmitted into the electromagnetic z wave.

In order to explain the present observations it is necessary to obtain a mechanism for exciting ion motions that can couple to the electron motions. The ion oscillations may be related to the observed enhancement of the nf_H resonances when $f_Z s \lesssim nf_H$. This enhancement, which has been reported earlier (Benson 1972a, 1974a) suggests that extra energy is fed into the longitudinal plasma waves associated with the nf_H resonance under these conditions. It has been observed on nf_H resonances with n as large as 9, it has not been observed on the f_H resonance (as discussed in connection with Figure 7), and it is difficult to determine if there is a definite enhancement of the $2f_H$ resonance when $f_Z S \lesssim 2f_H$ (which occurs when $f_N/f_H \lesssim 2.45$) since it has a peak time duration when $2 \lesssim f_N/f_H \lesssim 4$ (Benson, 1972a). The extra energy is attributed to wave mode coupling between the electromagnetic z wave and the longitudinal plasma wave associated with the nf_H resonance when $f_Z S \lesssim nf_H$. This coupling is possible because the dispersion curves directly connect under these conditions; a similar connection does not exist for the electromagnetic x wave (Shkarofsky, 1968).

The increased nf_H resonant time duration appears to be mainly dependent on the manner in which the extra energy is supplied to the medium, rather than on the amount of energy available, since an increase in the transmitted power from about 15W to 150W appears to have a negligible effect on the duration of the received signal (Benson, 1972a). It has been inferred from the observations that the longitudinal plasma oscillations associated with the higher order nf_H resonances are confined to the region of only a few meters around the sounder antenna (Benson, 1972a). This region is large compared to the ambient electron cyclotron radius (a few centimeters) but small compared to the ion cyclotron radius (tens of meters). One would expect the electromagnetic-electrostatic coupling process to extend over a region with dimensions at least as large as the electromagnetic wavelength (tens of meters). Longitudinal oscillations could then be initiated via wave-mode coupling over a region large enough to make ion effects important.

One may ask why spurs are not observed corresponding to the gyration time of ions other than hydrogen. Ionized hydrogen is the dominant ion above about 1000 km, but many of the spur observations correspond to lower altitudes where O^+ can be more abundant than H^+. The gyration time of O^+ is approximately 55 msec which greatly exceeds the duration of the nf_H resonances observed in this altitude range (Benson 1972a). Since the proton spur appears as a parasite attached to the host nf_H resonance (even the $6f_H$ spur of Figure 9b appears during the same general time frame as the main electron

resonance signal), the lack of O^+ spurs may be attributed to the relatively short resonant time duration of the host resonance. This argument is less convincing for the case of He^+ which is almost as abundant as H^+ (within an order of magnitude) in the altitude range of interest, and which has a gyration period (approximately 14 msec) which is within the duration time of some of the resonances.

In summary, the spurs on the nf_H resonances ($n = 2, 3, 4, \cdots$) appear to be related to a sounder stimulated Harris instability of the nf_H electron plasma waves in which ion motions are important. The observations indicate that the ion motions only become important when $f_Z S \lesssim nf_H$. This may be due to efficient coupling of energy from the z wave mode to the longitudinal nf_H plasma wave mode which then allows for the excitation of the longitudinal waves over a volume element large enough to sustain coherent ion oscillations. The resonance at f_H, which does not contain spurs, is not associated with waves that are susceptible to the Harris instability. Also, this resonance is not influenced by the z wave. The diffuse spurs on the $2f_H$ resonance when $f_N/f_H \approx 3$, and the proton effects observed on the diffuse resonances, may be related to an instability mechanism because the waves associated with these resonances are subject to the Harris instability (Oya, 1971). No mechanism is suggested for the small spurs often observed on the f_N resonances. The large spurs observed when $f_N \approx nf_H$ indicates that there may be a significant coupling of energy between different wave modes or a large increase in the radiation of energy into the medium under these conditions.

ACKNOWLEDGMENTS

The data used in this analysis were provided by the National Space Science Data center at the Goddard Space Flight Center. I am grateful to Mr. D. M. Verven and to Mr. J. M. Christian for their assistance in the data reduction, and to Dr. S. J. Bauer for helpful comments on the manuscript.

APPENDIX

The occasional observation of a spur overshoot to the high frequency side of a resonance (as in Figure 3), and the occasional nf_H spur observed to extend below the midpoint between nf_H and $(n-1)\,f_H$ are attributed to the wide bandwidth of the Alouette 2 sounder. The sounder uses a rectangular rf pulse of 100μsec duration, which gives rise to a sideband radiation pattern with nulls every 10 kHz on either side of the center frequency, and the receiver has a 3dB bandwidth of 37 kHz (Franklin and Maclean, 1969). An investigation of Alouette 2 ionograms (e.g., see Figures 1-4 and 7-9) indicates that the effective bandwidth for the detection of f_N, f_T and nf_H resonances is approximately 70 kHz. The overshoot to the high frequency side of the $4f_H$ resonance in Figure 3 is observed to be of this order or less. Similarly, the two nf_H spur observations of Figure 5 with f_{min}/f_H below the midpoint between nf_H and $(n-1)\,f_H$ can be explained in terms of the wide bandwidth since in both cases (the $4f_H$ spur with $f_{min}/f_H = 3.44$ and the $7f_H$ spur with $f_{min}/f_H = 6.44$) the f_{min} signal extends only 34 kHz into the lower half of the frequency domain between the harmonics of f_H.

Long spurs would not be observed on the nf_H resonances if the transmitted sounder energy was restricted to a narrow frequency range. Since the spurs are observed to be attached to the resonances, it is necessary to stimulate the resonance with energy radiated by the transmitter sidebands when the sounder is tuned to a lower frequency (where the spur is observed). The illustration of

Figure 4 indicates that when the sounder was tuned to the frequency indicated by the arrow labeled "a," there was sufficient sideband energy radiated at $2f_H$ (over 250 kHz away) to stimulate the $2f_H$ resonance. This sideband radiation can also initiate z wave propagation which appears to be necessary to stimulate the ion motion required for the spur generation. The maximum observed value for $f_z S - f_{min}$, from the data presented in Figure 5, is 366 kHz (corresponding to the $6f_H$ spur shown in Figure 9b). In this case the radiated energy at $f_z S$ is down by about 41 dB compared with the energy output at the sounder center frequency of f_{min}. Similar power levels have been proposed for the stimulation of plasma waves that take part in the non-linear wave-wave interaction process that produces diffuse resonances with time durations greater than a few milliseconds (Benson, 1974b).

REFERENCES

Benson, R. F. (1972a), Ionospheric plasma resonances: time durations vs. latitude, altitude, and f_N/f_H, Planet. Space Sci., 20, 683-706.

Benson, R. F. (1972b), Frequency shifts of ionospheric nf_H resonances, J. Atmos. Terr. Phys., 34, 1201-1214.

Benson, R. F. (1974a), Stimulation of the Harris Instability in the ionosphere, Phys. Fluids, 17.

Benson, R. F. (1974b), On the generation of the sequence of diffuse resonances observed on topside ionograms, J. Geophys. Res., 79.

Franklin, C. A., and M. A. Maclean (1969), The design of swept-frequency topside sounders, Proc. IEEE, 57, 897-929.

Graff, P. (1967), Influence de la gyrofrequence protonique sur la resonance d'une antnna a la frequence du plasma electronique, Compt. Rend., 265 B, 618-620.

Harris, E. G. (1959), Unstable plasma oscillations in a magnetic field, Phys. Rev. Letters, 2, 34-36.

Harris, E. G. (1964), The electron cyclotron instability, General Atomic Report GA-5581.

King, J. W., and D. M. Preece (1967), Observations of proton gyro-effects in the top-side ionosphere, J. Atmos. Terr. Phys., 29, 1387-1390.

Matuura, N, R. Nishizaki (1969), Proton cyclotron echoes in the topside ionosphere, J. Geophys. Res., 74, 5169-5172.

Muldrew, D. B. (1972), Electron resonances observed with topside sounders, Radio Sci., 7, 779-789.

Oya, H. (1971), Verification of theory on weak turbulence relating to the sequence of diffuse plasma resonances in space, Phys. Fluids, 14, 2487-2499.

Palmer, F. H., and R. E. Barrington (1973), Excitation of ion resonances by the Isis 2 HF Transmitter, J. Geophys. Res., 78, 8167, 8179.

Shima, Y., and L. S. Hall (1965), Electrostatic instabilities in a plasma with anisotropic velocity distribution, Phys. Rev., 139, A1115-A1116.

Shkarofsky, I. P. (1968), Higher Order Cyclotron Harmonic Resonances and their Observation in the Laboratory and in the Ionosphere, J. Geophys. Res., 73, 4859-4867.

Stix, T. H. (1962), The theory of plasma waves, p. 227, McGraw-Hill, Inc., New York.

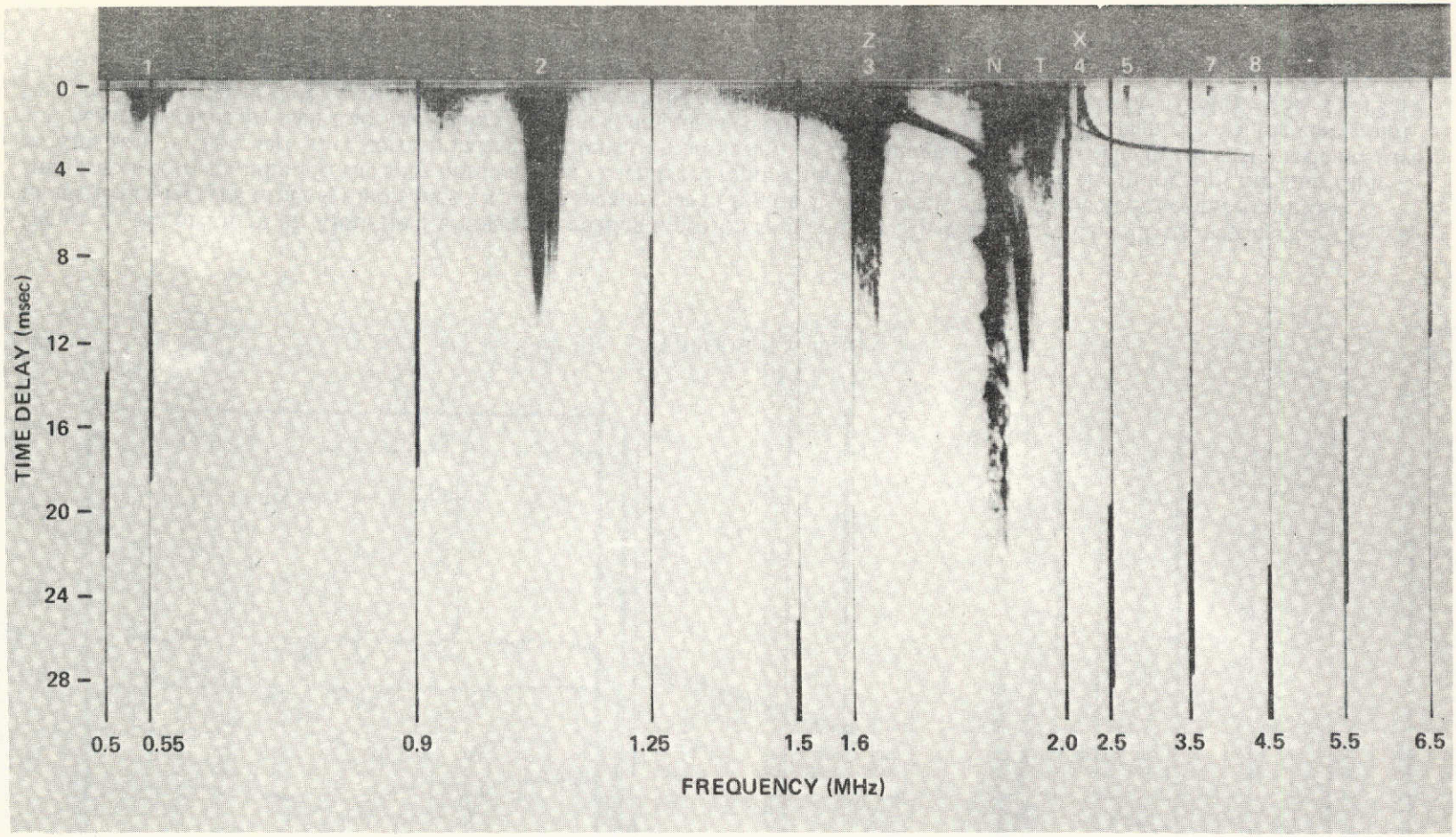

Figure 1. A portion of an Alouette 2 ionogram revealing multiple proton spurs on the resonance at the electron plasma frequency (designated by N). The resonance at the upper-hybrid frequency is identified by T and the resonances at f_H, $2f_H$, $3f_H \cdots$, by 1, 2, 3, $\cdots$. The satellite cutoff frequencies $f_Z S$ and $f_X S$ for the z and x waves of the electromagnetic extraordinary mode are labeled Z and X, respectively. (QUI pass 1726, 23 April 1966, 20:23:20 UT; 4.8° S, 66.2° W, 1002 km.)

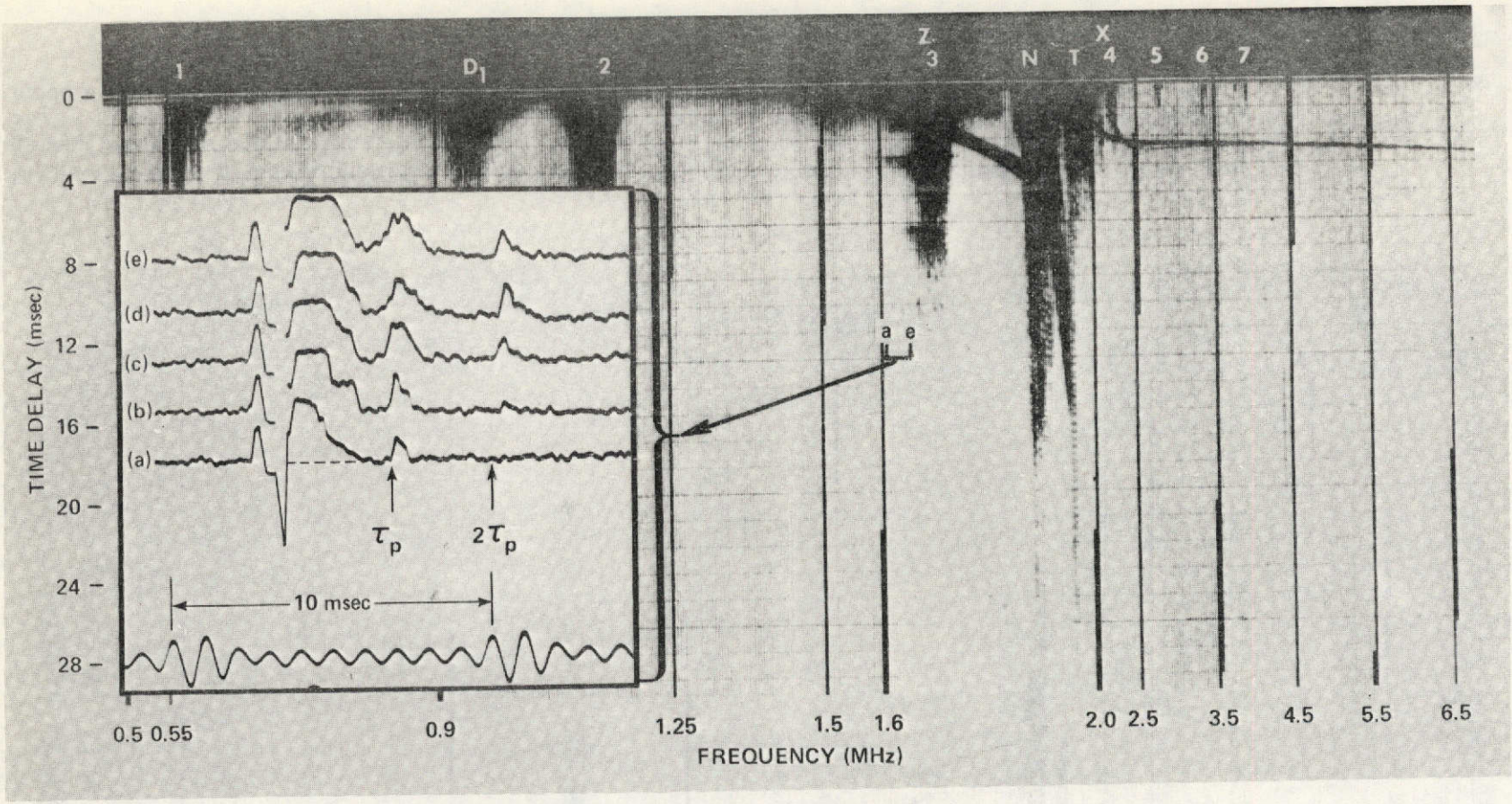

Figure 2. A portion of an Alouette 2 ionogram revealing 2 proton spurs on the $3f_H$ resonance. The diffuse resonance at f_{D1} is identified as D_1; the other symbols have the same meaning as in Figure 1. The insert shows 5 selected receiver amplitude vs. time traces corresponding to the spur observations. Each trace represents a vertical scan line on the ionogram; the amplitude modulation on the insert trace corresponding to intensity modulation on the ionogram scan line. The initial systematic positive and negative spikes on each trace are calibration and sync pulses (see Figure 31 of Franklin and Maclean, 1969); the zero point for measuring receiver delay was taken at the left edge of the dashed line on trace (a). (SNT pass 1927, 10 May 1966, 19:12:17 UT; 21.4° S, 81.7° W, 791 km.)

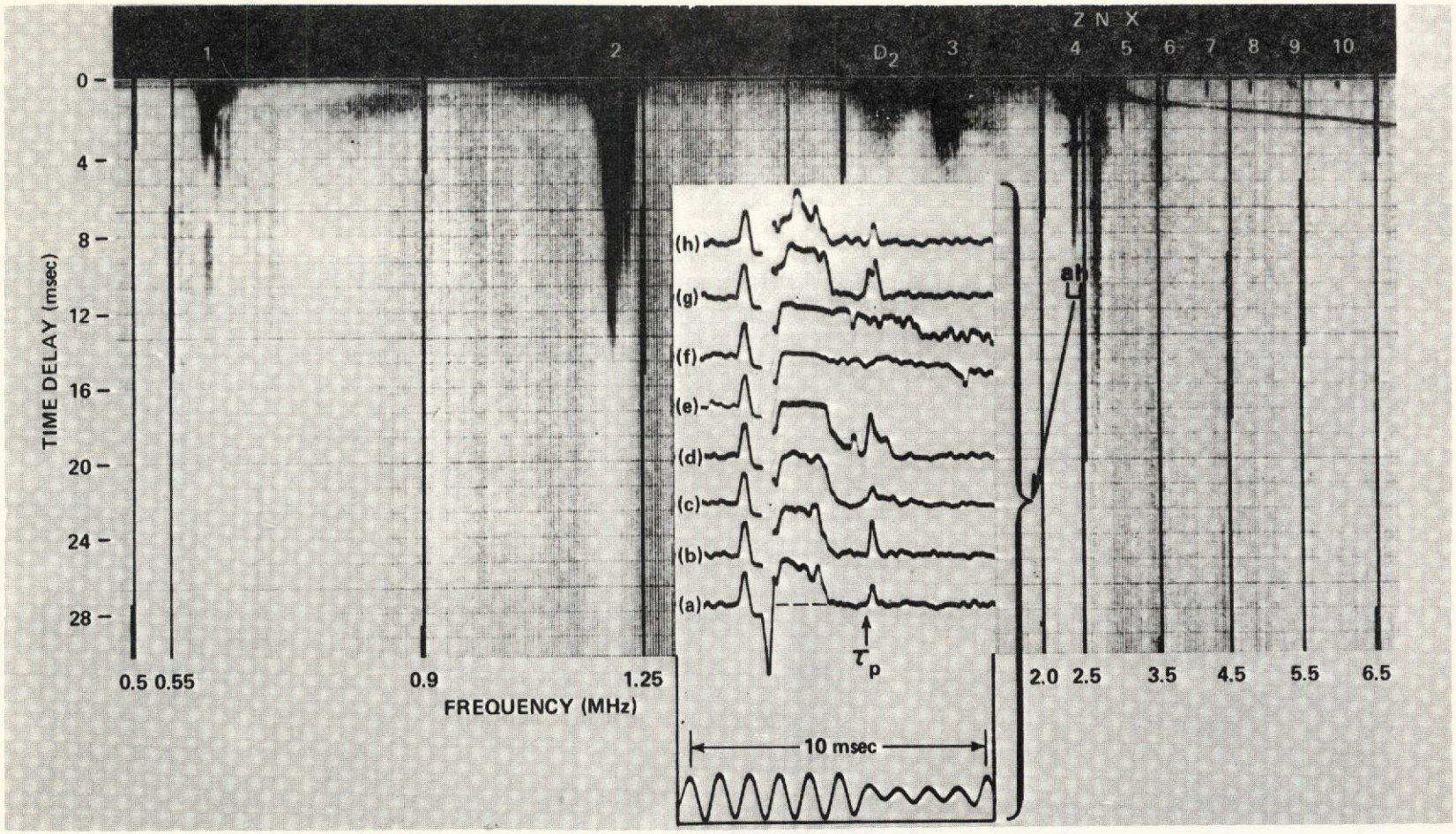

Figure 3. A portion of an Alouette 2 ionogram, with an insert containing 8 consecutive receiver amplitude vs. time traces, revealing a proton spur on the $4f_H$ resonance which overshoots to the high frequency side of the resonance. The diffuse resonance at f_{D2} is identified as D_2; the other symbols have the same meaning as in Figure 1. (SNT pass 1927, 10 May 1966, 19:14:57 UT; 11.1°S, 80.4°W, 678 km.)

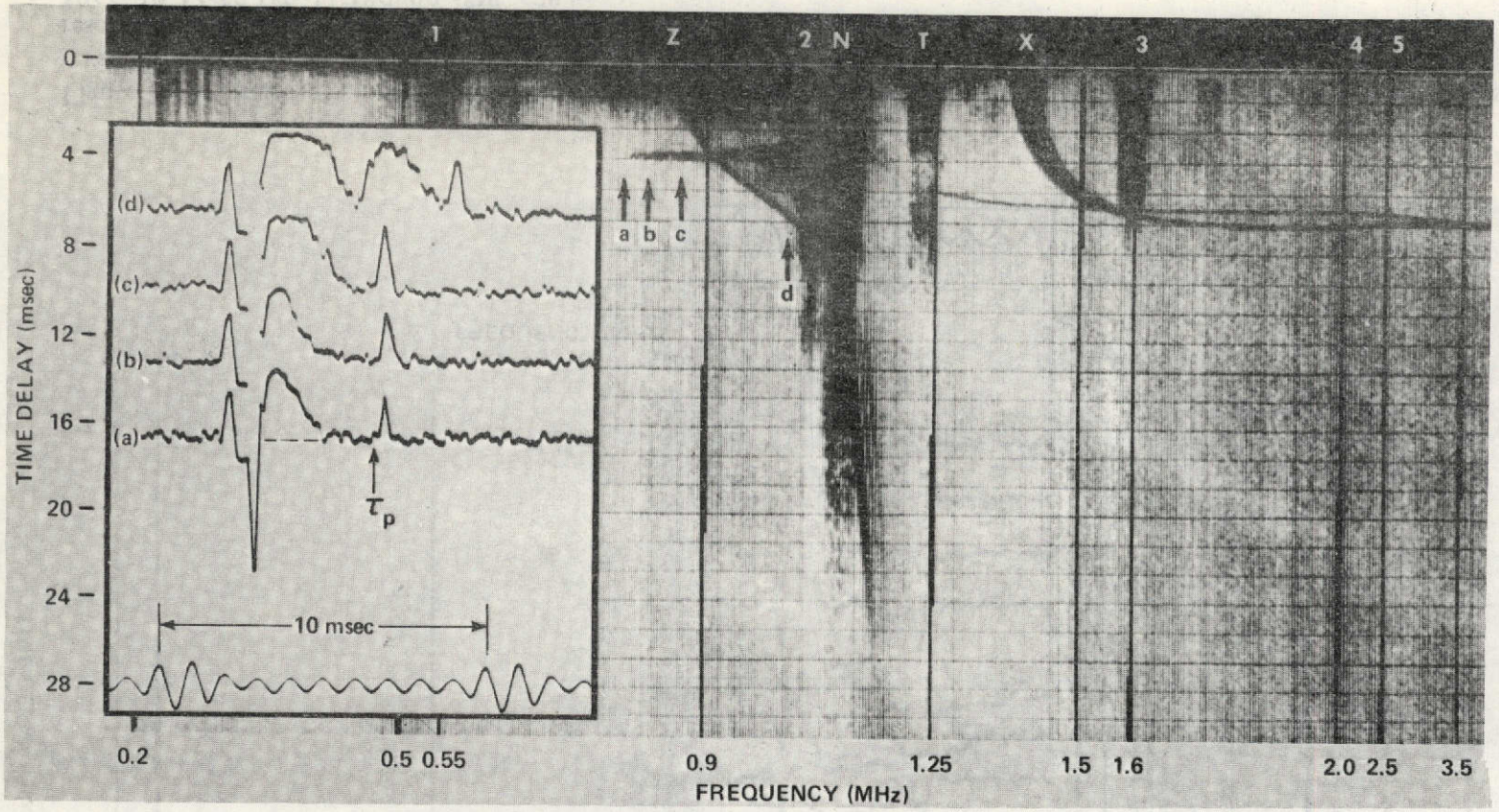

Figure 4. A portion of an Alouette 2 ionogram, with an insert containing 4 selected receiver amplitude vs. time traces, revealing a large proton spur on the combined $2f_H$, f_N resonance. The trace labeled (a) is the first one with a significant spur signal; the trace labeled (d) shows a broadened spur signal followed by an ionospheric echo from the electromagnetic z wave. (SNT pass 4086, 8 November 1966, 21:39:15 UT; 34.0° S, 84.9° W, 1236 km.)

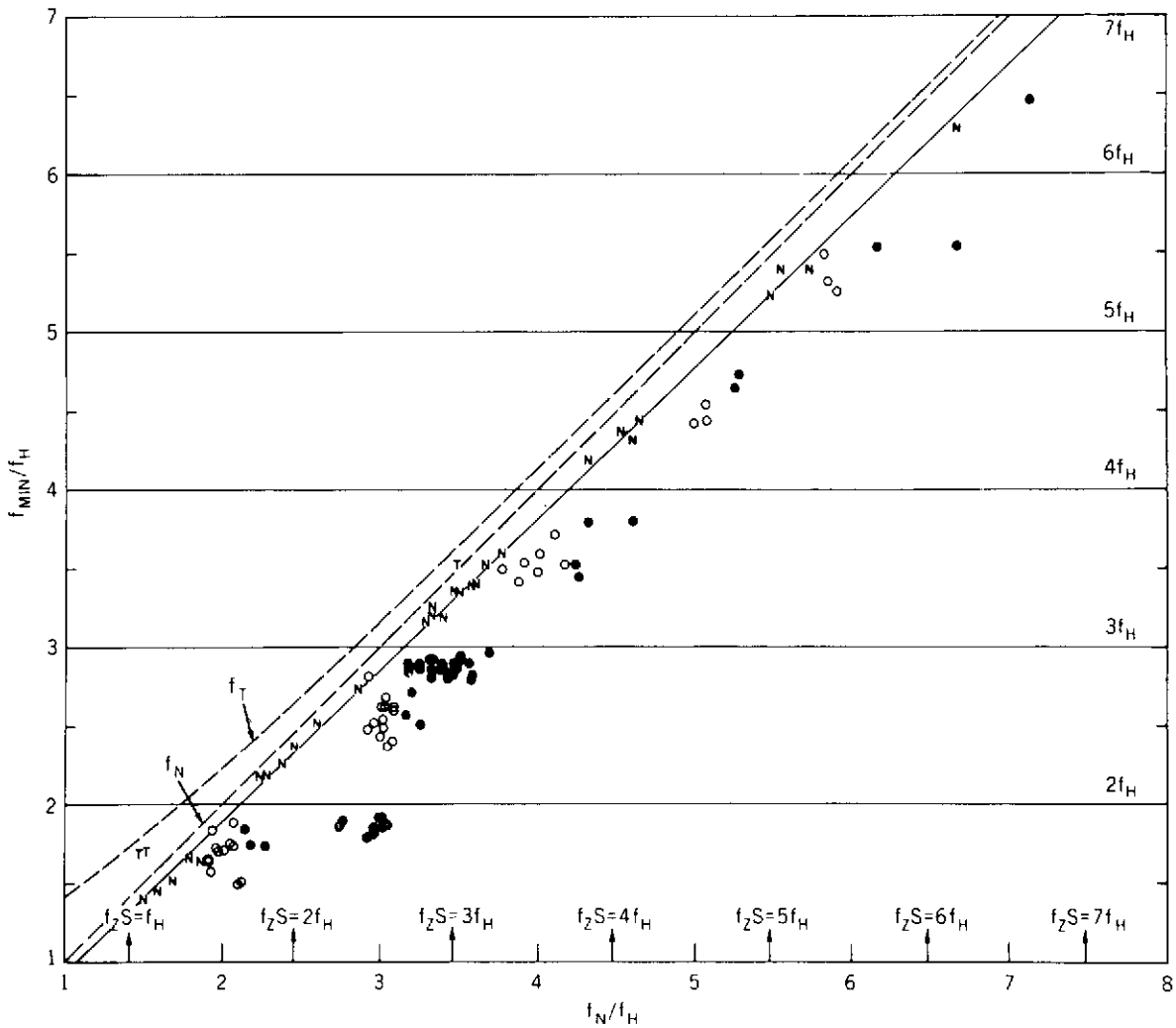

Figure 5. The minimum observed proton spur frequency f_{min} (normalized by f_H) as a function of f_N/f_H. The symbols N, T, solid circle, and open circle represent proton spurs on the f_N resonance, the f_T resonance, the nf_H resonances, and the resonance resulting from the overlap of f_N with nf_H, respectively. For example, the open circle at $f_N/f_H = 2.10$ and $f_{min}/f_H = 1.50$ corresponds to the spur presented in Figure 4. The lines labeled f_N, f_T, $2f_H$, $3f_H \cdots$, correspond to the indicated resonance when no spur is observed. The slanting solid line represents a least squares fit to the N's. The vertical arrows at the bottom of the figure indicate the conditions where $f_z S = nf_H$; the frequency region to the left of the arrow corresponds to $f_z S < nf_H$.

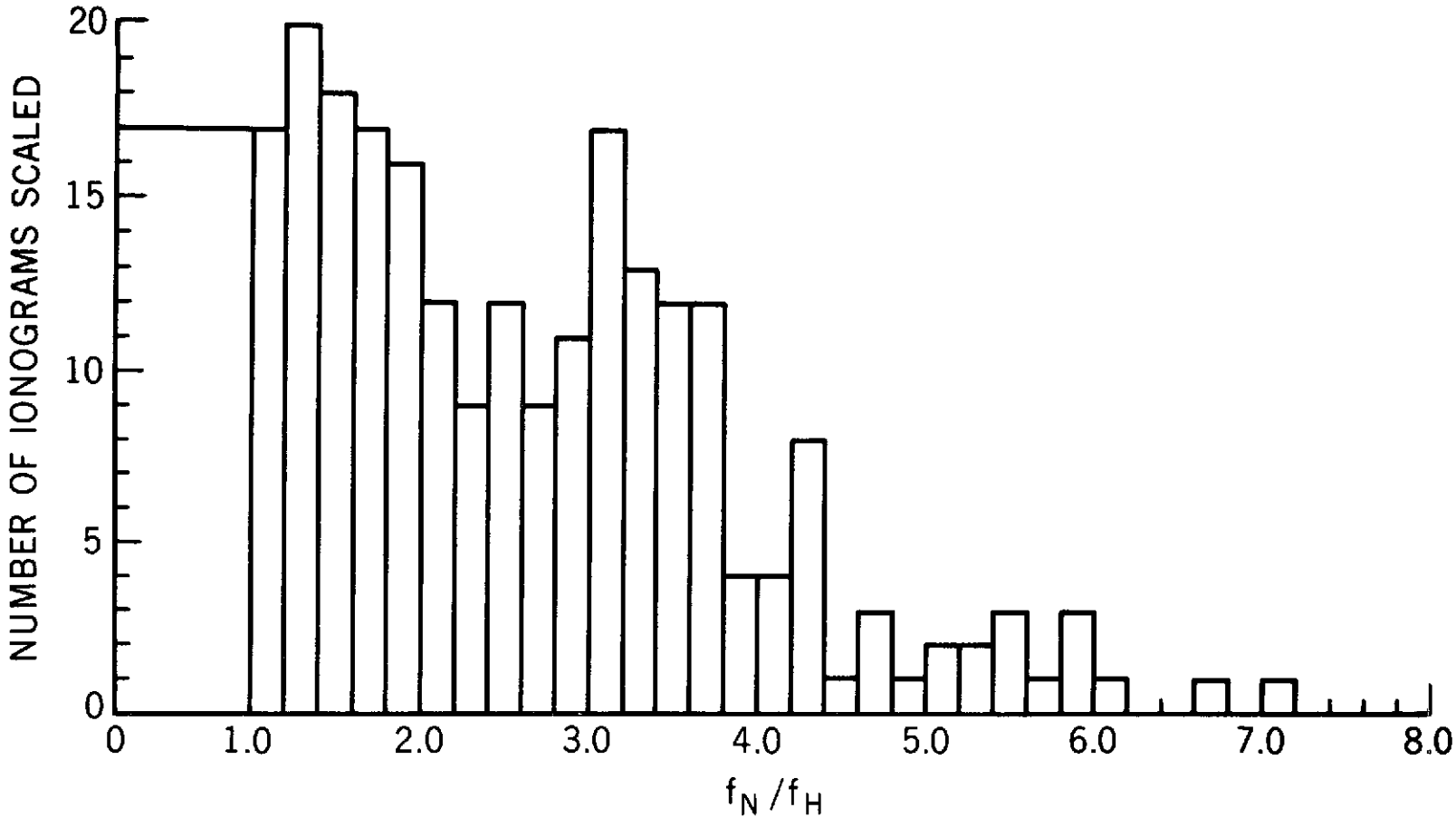

Figure 6. Number of Alouette 2 ionograms scaled as a function of f_N/f_H corresponding to the proton spur observations of Figure 5.

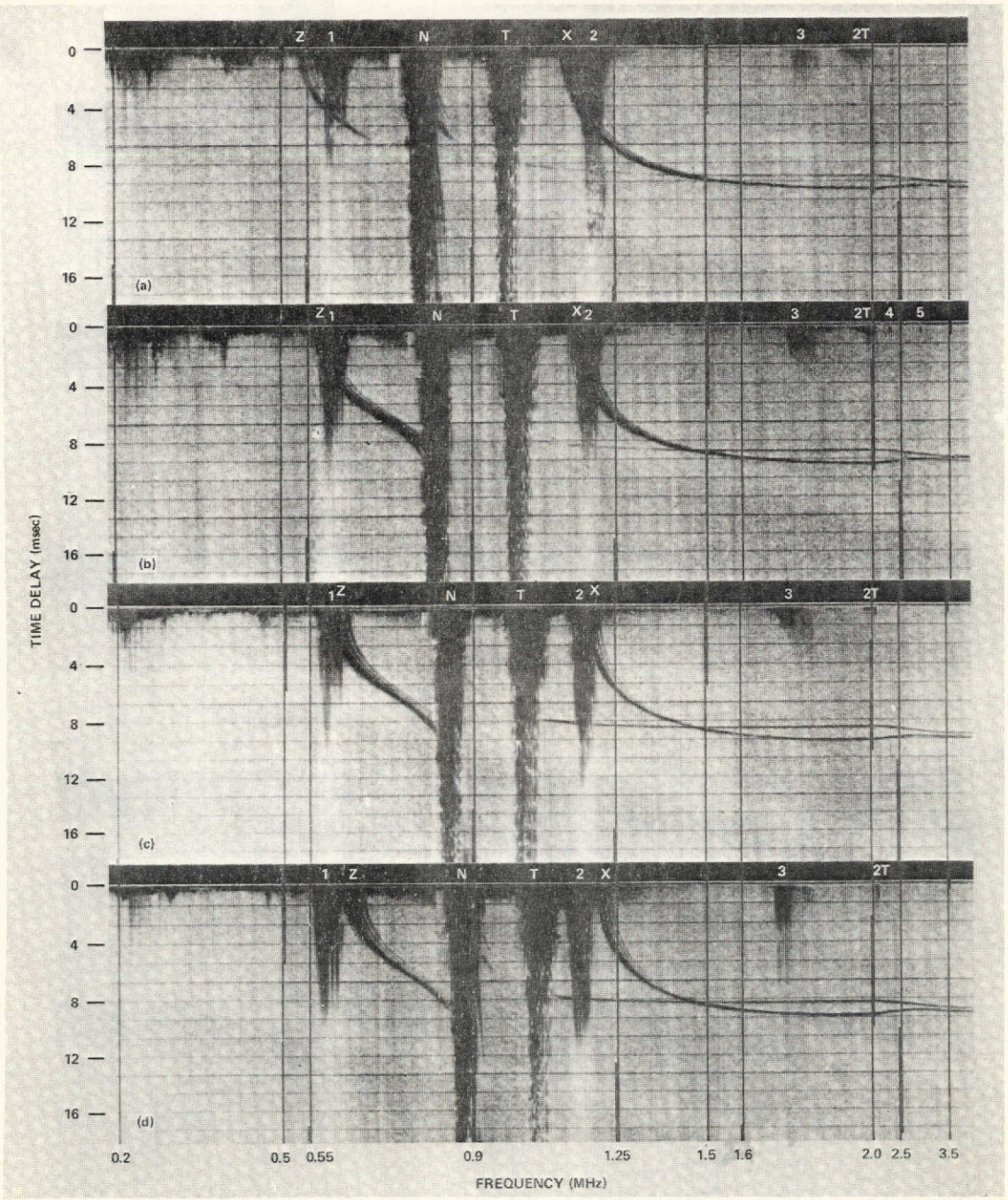

Figure 7. Portions of 4 consecutive Alouette 2 ionograms showing the transition of $f_z S$ through f_H. The symbol 2T refers to the resonance at $2f_T$; the other symbols are the same as in Figure 1. (SNT pass 4086, 8 November 1966, 21:33:34 UT (a) to 21:35:07 UT (d); 51.7° S (a) to 47.0° S (d), 89.6° W (a) to 87.9° W (d), 1608 km (a) to 1505 km (d).)

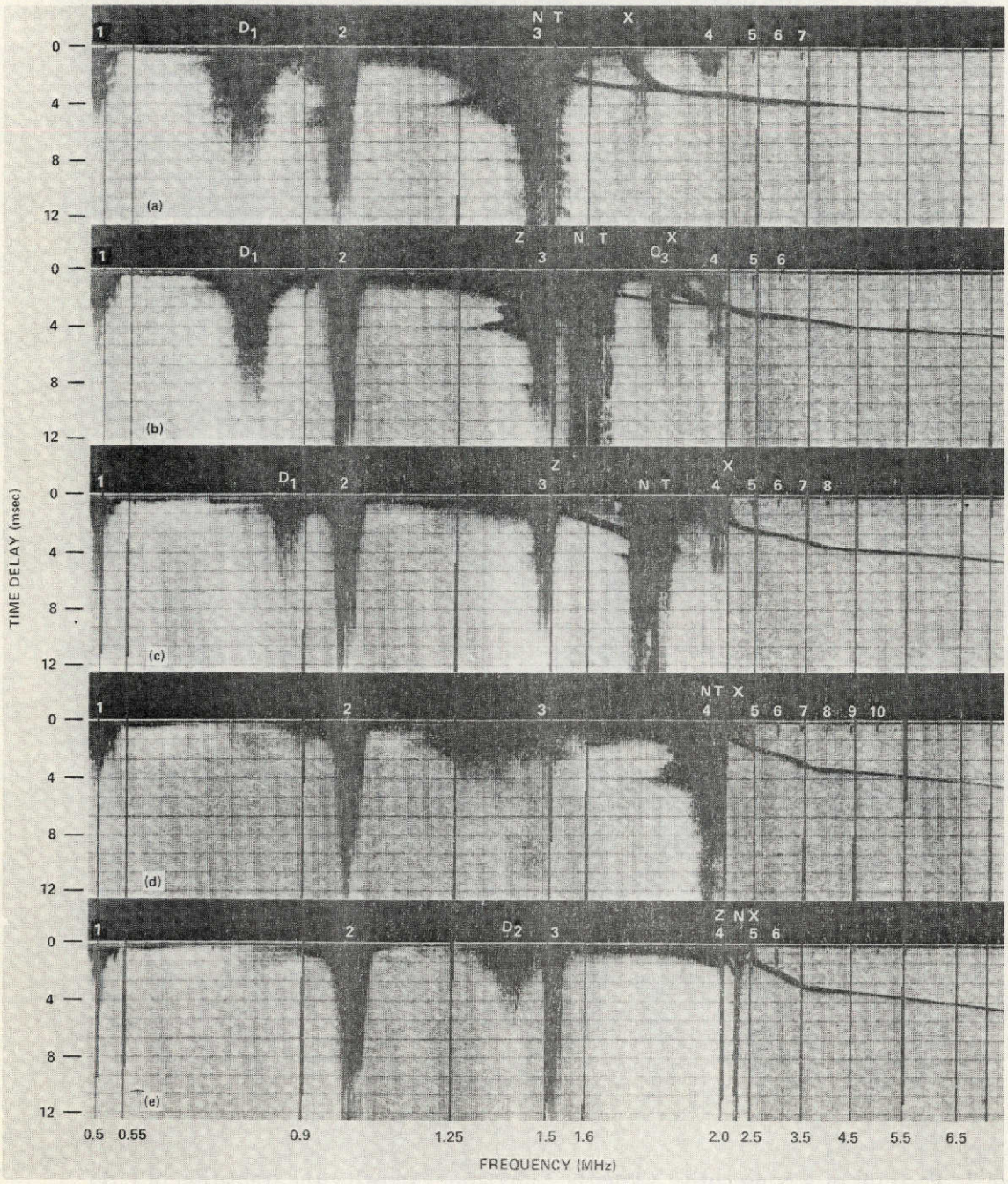

Figure 8a-e. See caption for Figure 8f-i.

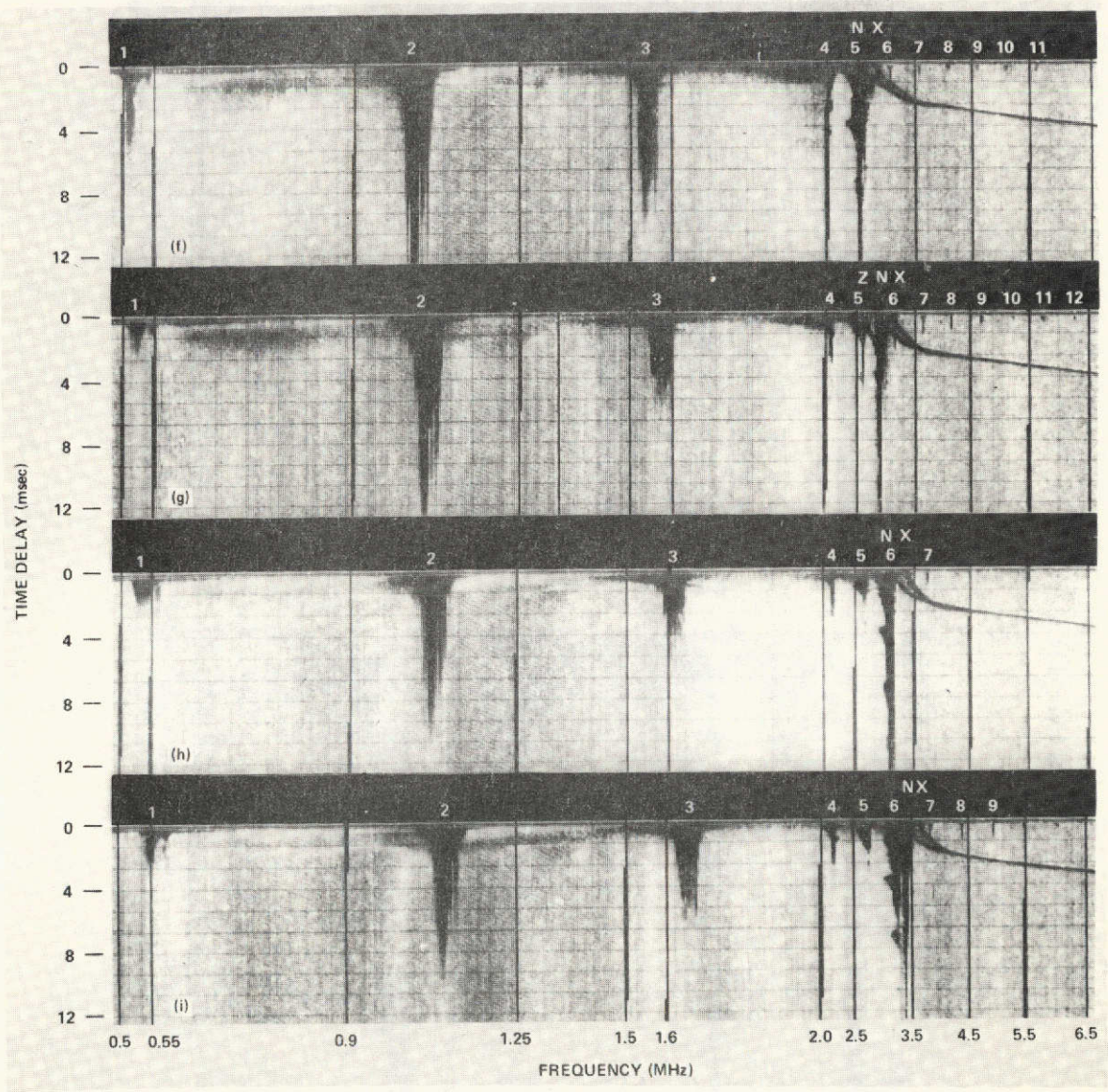

Figure 8f-i. Nine consecutive ionograms (Figure 8a-8i) representing changing resonance and spur characteristics due to the variations in electron density. (SNT pass 1844, 3 May 1966, 19:10:04 UT (a) to 19:14:14 UT (i); 25.3° S (a) to 10.7° S (i), 69.6° W (a) to 67.6° W (i), 1039 km (a) to 813 km (i).)

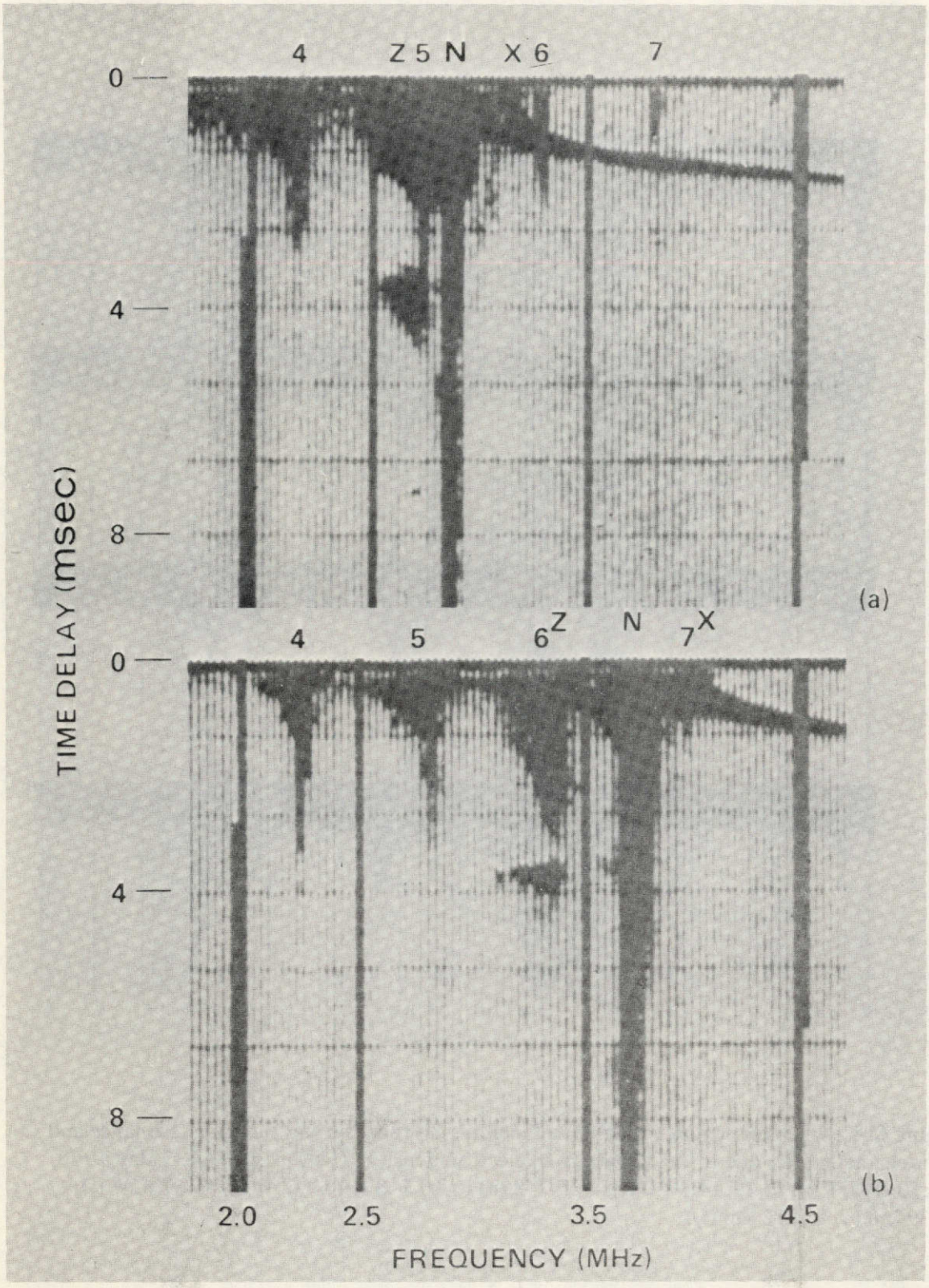

Figure 9. Proton spur observed on the $5f_H$ resonance in (a) and the $6f_H$ resonance in (b). (SNT Alouette 2 pass 1962, 13 May 1966, 18:03:52 UT (a) and 18:04:56 UT (b); 18.3° S, 68.5° W, 705 km for (a); 15.3° S, 68.9° W, 663 km for (b).)

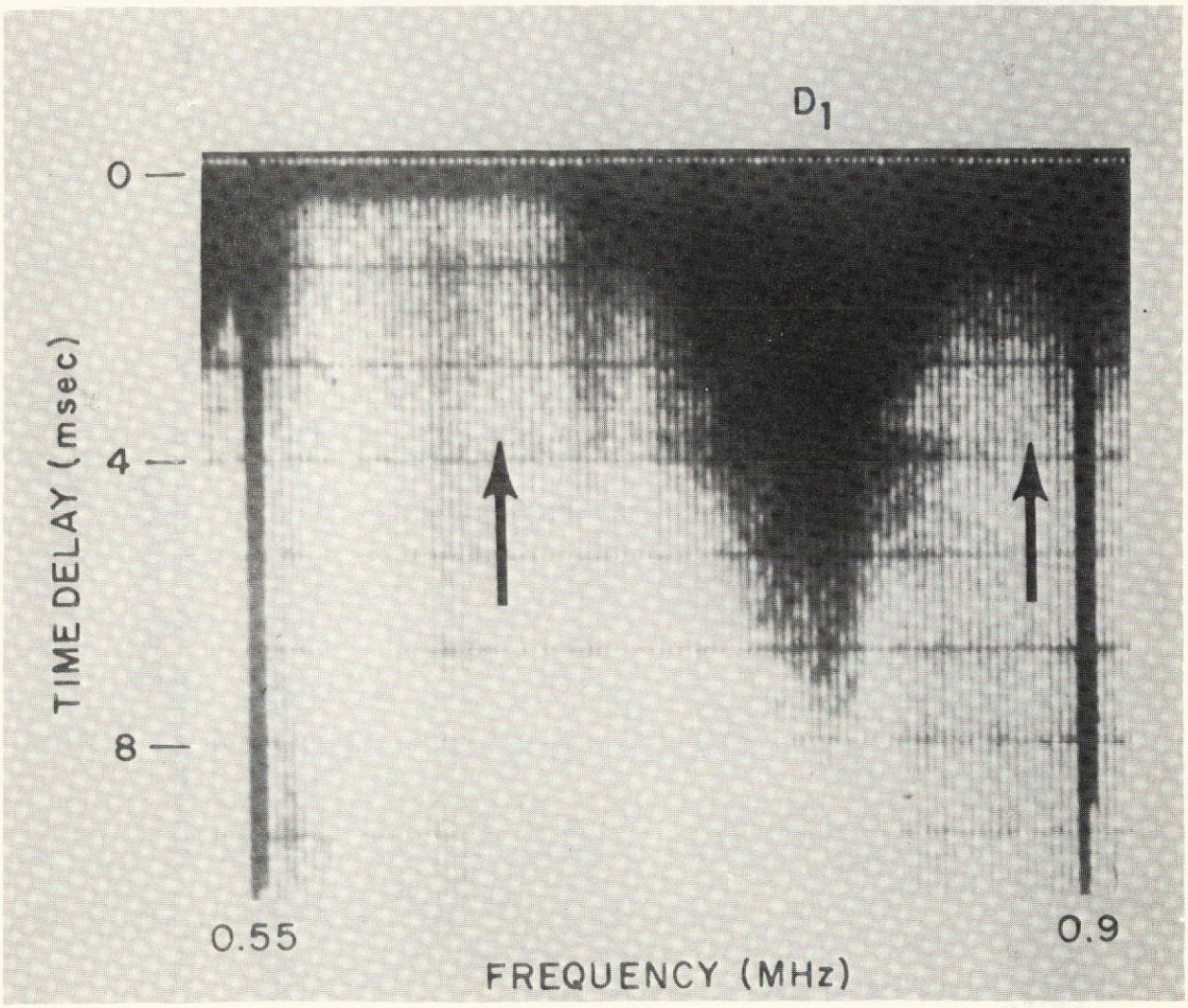

Figure 10. Proton signal on the f_{D1} diffuse resonance. The vertical arrows identify the lower and upper frequency limits of the proton signal as observed on the ionogram film. The proton signal is a thin trace connecting the tips of the arrows. (SNT Alouette 2 pass 4086, 8 November 1966, 21:41:19 UT; 27.0° S, 83.7° W, 1107 km.)

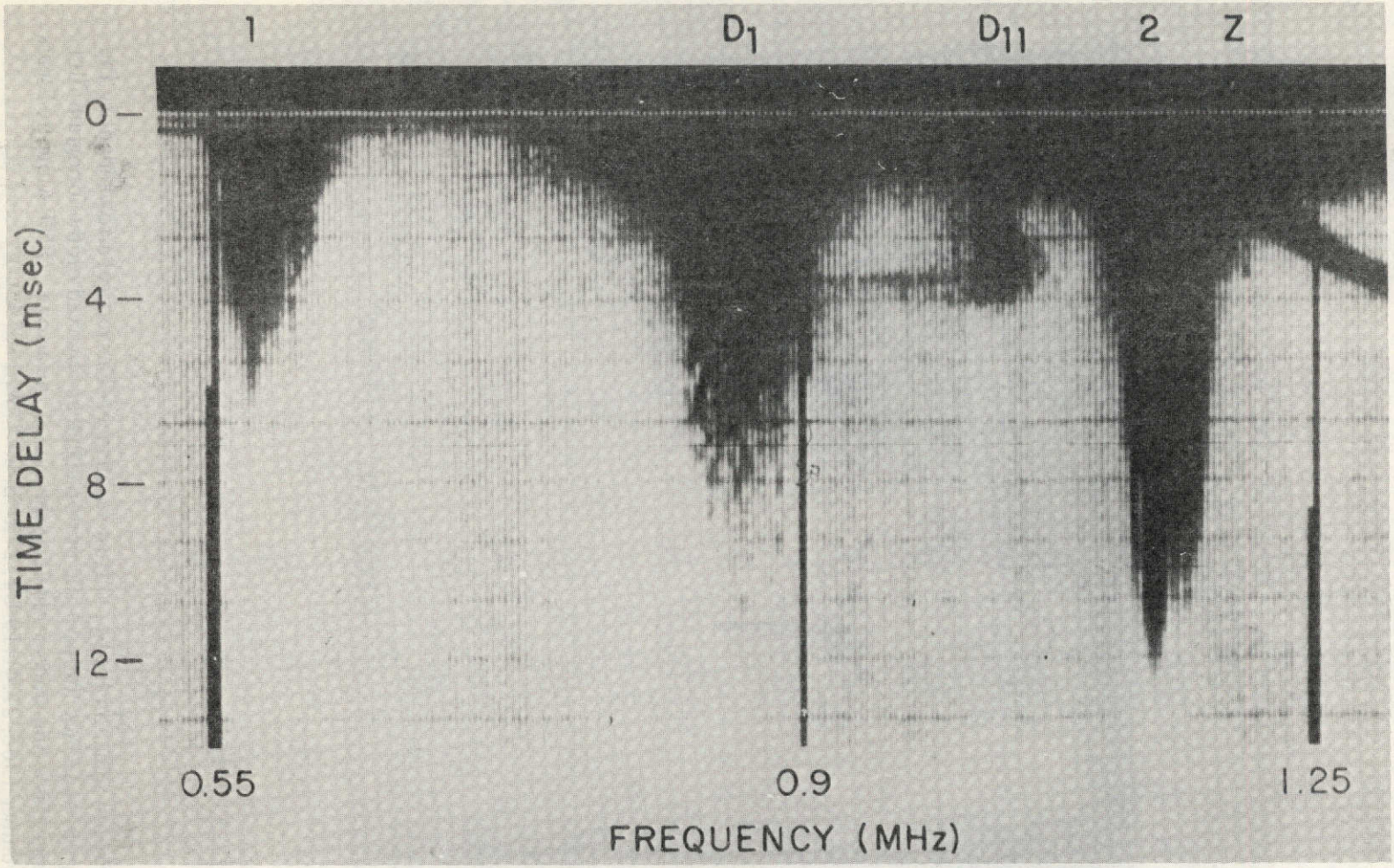

Figure 11. Proton signal on the $f_{D\,11}$ diffuse resonance. (SNT Alouette 2 pass 1927, 10 May 1966, 19:10:09 UT; 29.4° S, 82.9° W, 901 km.)

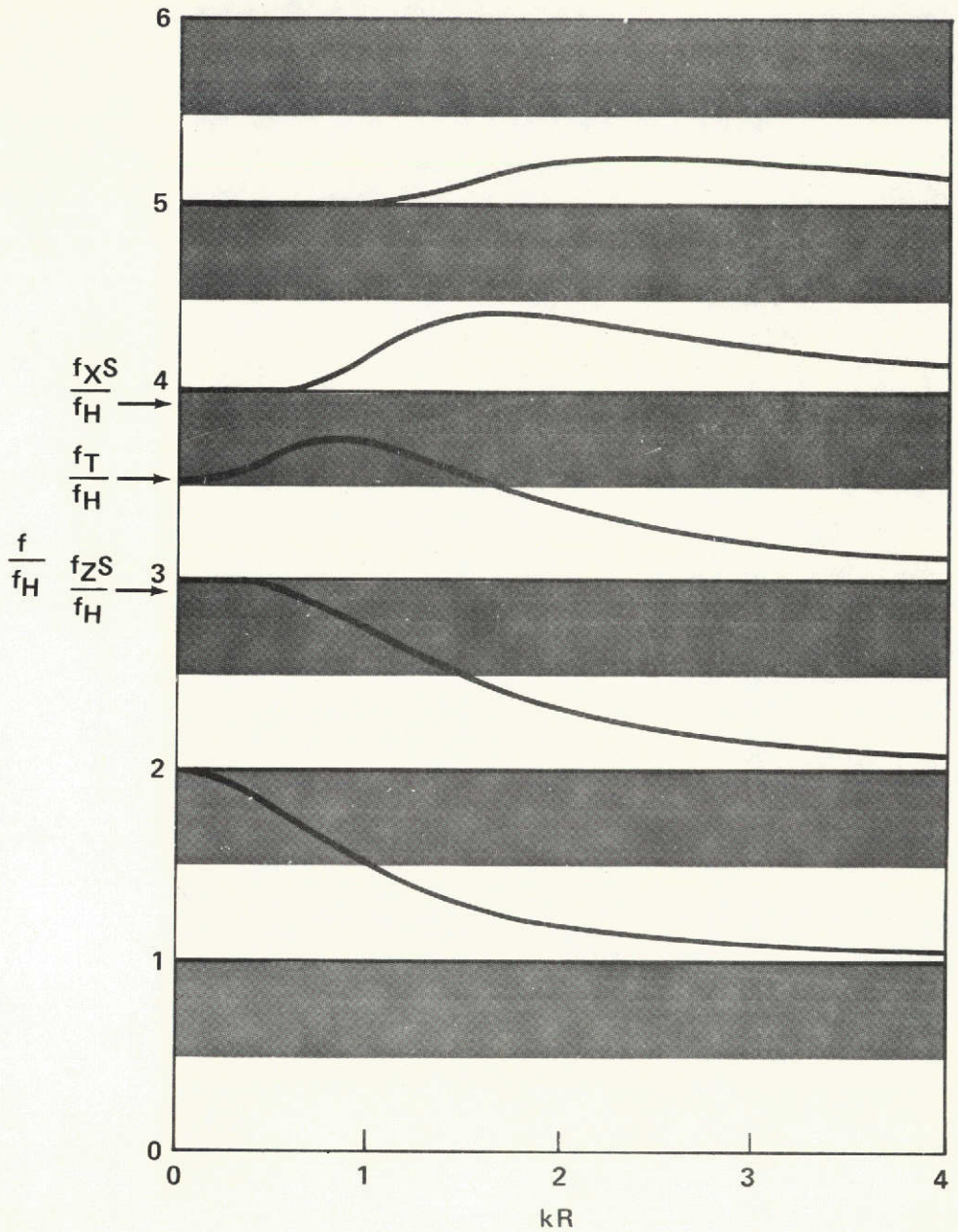

Figure 12. The normalized dispersion curves for plasma waves propagating perpendicular to $\vec{B}$ (Stix, 1962). The wave number k is normalized by the inverse of the electron cyclotron radius R. The shaded regions indicate where the Harris instability can be stimulated for oblique propagation. The changes in the low kR portion of the dispersion curves near $f/f_H \approx n$ are very minor as the propagation deviates from the perpendicular direction (Oya, 1971).